Ordered Assemblies

DOI: 10.1002/anie.200803642

Ordered Gold Nanostructure Assemblies Formed By Droplet Evaporation**

Tian Ming, Xiaoshan Kou, Huanjun Chen, Tao Wang, Hoi-Lam Tam, Kok-Wai Cheah, Ji-Yao Chen, and Jianfang Wang**

Ordered assemblies of anisotropic nanostructures have attracted increasing interest because of the rich assembling behavior caused by their reduced shape symmetry and the unique collective properties that can be engineered by controlling interparticle spacing and by material processing. The formation of columnar superstructures has been reported for gibbsite[1] and copper sulfide platelets.[2] Beautiful iridescent liquid-crystalline phases (nematic or smectic) have been reported for suspensions of rodlike particles, including DNA,[3] viruses,[4] $BaCrO_4$,[5] β-FeOOH,[6] TiO_2,[7,8] and CdSe.[9] Semiconductor nanorods with interesting optical properties are useful for device applications (light-emitting diodes, memory devices, and solar cells), and efforts have been made to produce large-area ordered semiconductor nanorod superstructures. One approach that has been developed is the deposition of preformed nanorod liquid crystals from suspensions onto substrates. Ordered solid assemblies of CdS and CdSe nanorods have been obtained in this way.[10–12] Onsager's theory[13] stated that suspensions of hard rods that have zero interaction potential until they touch, at which point they infinitely repel each other, exhibit the nematic phase at critical densities far from the closest packing. In real colloidal systems, attractive van der Waals and dipole–dipole and repulsive electrostatic interactions also influence the liquid-crystalline phase behavior.

Noble metal nanostructures exhibit shape- and size-dependent plasmonic properties, which can be controlled over a wide spectral range. The electric field close to the surface of metal nanostructures is largely enhanced when they are resonantly excited. Metal nanostructure assemblies can therefore be employed for the amplification of optical signals (fluorescence, Raman, and absorption spectroscopies). Ordered assemblies of rodlike Au nanostructures have been obtained by slowly drying aqueous dispersions of Au nanostructures.[14–18] However, the lateral sizes and heights of the resultant assemblies are limited to a few micrometers and several layers, respectively. Droplet evaporation has recently been widely recognized as a nonlithographic route to generate regular patterns of solutes dispersed in solvents. Such patterns are known as "coffee ring" patterns, which form when nonvolatile solutes are carried to the pinned droplet edge by outward flowing of solvents from the interior to the edge.[19–22] Materials out of which intriguing assemblies and patterns have been produced by droplet evaporation include DNA,[23] porphyrin trimers,[24] conjugated polymers,[25,26] colloidal silica spheres,[27] noble metal nanoparticles,[28–30] semiconductor nanocrystals and nanorods,[31–33] and carbon nanotubes.[34]

Herein, we report on the generation of ordered assemblies of Au nanostructures by solvent evaporation of a droplet of aqueous dispersions of Au nanostructures at high concentrations. The resultant assemblies form a ring 2–5 mm in diameter and 15–50 μm in width (0.1–0.8 mm^2 in area), with a depth of 1.7–2.2 μm. The assembled superstructures are shape-dependent, with Au nanorods, polyhedra, nanocubes, and bipyramids exhibiting nematic/smectic-A, hexagonally packed, tetragonally packed, and nematic/three-dimensionally (3D) ordered superstructures, respectively. When Au nanostructures of two different sizes or shapes are mixed together at a 1:1 molar ratio, binary mixtures of Au nanorods form nematic superstructures, or self-separate to form smectic superstructures, depending on their relative sizes. Binary mixtures of Au nanorods and polyhedra form an alternating ordered superstructure. Confocal laser scanning microscopy measurements have further shown that the two-photon-excited luminescence intensity of ordered Au nanorod superstructures is several times larger than that of disordered Au nanorod assemblies.

Gold nanostructures of different sizes and shapes, including nanorods, polyhedra, nanocubes, and bipyramids, were prepared using the seeded growth method described previously.[35–41] As-prepared Au nanostructures are stabilized in 0.1M cetyltrimethylammonium bromide (CTAB) aqueous dispersions, except the bipyramids, which are stabilized in 0.01M cetyltributylammonium bromide (CTBAB). Their particle concentrations are approximately 1.0 nM in aqueous dispersions. The concentrations of the stabilizing surfactants and Au nanostructures were adjusted by centrifugation and

[*] T. Ming, X. S. Kou, H. J. Chen, Prof. J. F. Wang
Department of Physics, The Chinese University of Hong Kong
Shatin, Hong Kong SAR (China)
Fax: (+852) 2603-5204
E-mail: jychen@fudan.edu.cn
T. Wang, Prof. J.-Y. Chen
Surface Physics Laboratory (National Key Laboratory)
and Department of Physics, Fudan University
Shanghai 200433 (China)
Fax: (+86) 21-6510-4949
E-mail: jfwang@phy.cuhk.edu.hk
Dr. H.-L. Tam, Prof. K.-W. Cheah
Department of Physics, Hong Kong Baptist University
Kowloon Tong, Hong Kong SAR (China)

[**] This work was supported by the RGC Research Grant Direct Allocation (Project Code: 2060332) and the NSFC/RGC Joint Research Scheme (Ref. No.: N_CUHK448/06, Project Code: 2900318).

Supporting information for this article is available on the WWW under http://dx.doi.org/10.1002/anie.200803642.

redispersion to roughly 3 mM and 20 nM, respectively. One drop (typically 10 μL) of each Au nanostructure dispersion was cast onto a silicon substrate and dried in air. During drying, the contact line of the droplet undergoes stick-slip motion, that is, little movements interspersed with large and rapid displacements, as a result of competition between the pinning and capillary forces,[19–22] leaving a small amount of Au nanostructures ($< 50\ \mu m^{-2}$) distributed randomly on the substrate (Figure S1 in the Supporting Information). Concurrently, the concentration of gold nanostructures is gradually increased, as a result of solvent evaporation. When the contact line is pinned (fixed), the solvent evaporating from the edge is replenished by solvent from the interior. The outward solvent flow carries dispersed Au nanostructures to the edge.[19–22] As a result, the concentration of Au nanostructures at the edge is higher than that at the center. When the nanostructure concentration at the edge increases up to a certain point, liquid-crystalline phases of Au nanostructures start to form out of the isotropic dispersions. The resultant liquid-crystalline phases precipitate to the substrate at the edge, which helps to pin the contact line (Figure 1 a). As more Au nanostructures are carried to the edge by the outward solvent flow, the liquid-crystalline phases grow larger. When the contact angle decreases to a critical value, owing to the continuous solvent evaporation, the contact line starts to recede until the solvent is completely evaporated. During this process, a ring with ordered assemblies of Au nanostructures is left on the substrate. Inside the ring are disordered nanostructure assemblies, which are a few layers in thickness. The surface density of Au nanostructures inside the ring decreases slowly with increasing proximity to the center of the ring (Figure S1 and S2 in the Supporting Information).

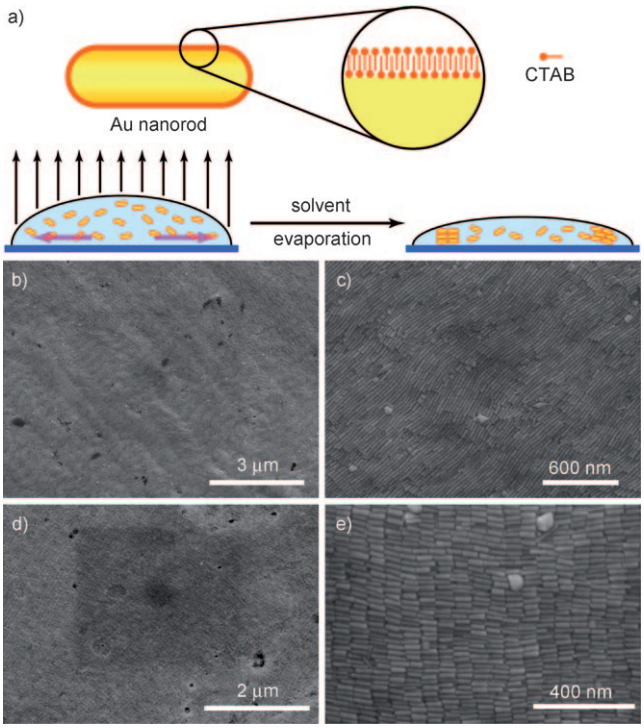

Figure 1. a) Schematic showing a Au nanorod stabilized by a cetyltrimethylammonium bromide (CTAB) bilayer, and the droplet-evaporation-induced formation of ordered Au nanorod superstructures; b) low-magnification SEM image of the nematic Au nanorod (AR = 4.4) superstructure; c) Au nanorod (AR = 4.4) superstructure SEM image at higher magnification; d) low-magnification SEM image of the smectic-A Au nanorod superstructure; e) smectic-A Au nanorod superstructure SEM image at higher magnification.

Ordered assemblies of Au nanostructures were investigated using scanning electron microscopy (SEM). Figure 1 b–e show the SEM images of the superstructures formed from Au nanorods [diameter = (17 ± 2) nm, length = (75 ± 6) nm, aspect ratio (AR) = 4.4 ± 0.7, longitudinal surface-plasmon-resonance wavelength (SPRW) = 862 nm] at different magnifications. The nanorods assemble into either nematic or smectic-A phases. The nanorods in the nematic structure assemble together in an end-to-end fashion to form chains and the chains pack, nearly parallel to each other, into a 3D structure. In the smectic-A structure, the nanorods assemble together in a side-by-side fashion to form layers and the layers pack nearly parallel to each other into a 3D structure. The fast Fourier transform of the smectic-A structure shows diffuse streaks corresponding to both the side-by-side alignment of Au nanorods and the periodically stacked layers that are perpendicular to the nanorod length axis, whereas that of the nematic structure shows diffuse streaks corresponding to the parallel alignment of the chains of nanorods and a nearly periodic, wavy corrugation with a larger periodicity (Figure S3 in the Supporting Information). Such nematic and smectic superstructures were also formed by smaller Au nanorods. For example, Figure S4 in the Supporting Information shows the nematic and smectic superstructures formed from Au nanorods with an average diameter, length, AR, and longitudinal SPRW of (11 ± 2) nm, (42 ± 4) nm, 3.8 ± 0.4, and 786 nm, respectively. Shorter Au nanorods often align vertically. The fast Fourier transform reveals that Au nanorods are nearly hexagonally packed within each layer of the smectic superstructure. In addition, the sizes of the individual nematic and smectic domains obtained from the droplet-evaporation technique can be as large as 100 μm^2. However, conditions for the formation of only one type of nanorod superstructure, either nematic or smectic, are yet to be discovered.

Cationic stabilizing surfactants play an important role in the formation of ordered nanorod superstructures by droplet evaporation. In our experiments, when as-prepared nanorod solutions are drop-cast onto substrates, excess cationic surfactants and nanorods phase-separate and form their own ordered structures. The resultant nanorod superstructures are coated with surfactant crystals, making SEM imaging difficult owing to electrostatic charge. Excess surfactants are therefore removed by centrifugation to avoid their deposition on the substrate. However, the surfactant concentration in the nanorod dispersions has to be larger than a critical value for the formation of ordered superstructures. For nanorods with AR = 4.4, the critical CTAB concentration was approximately 1.0 mM. Below this concentration, disordered nanorod assemblies were observed in the ring annulus (Figure S5a in the Supporting Information). This critical concentration appears to correspond to the amount of surfactant required to form a bilayer on the nanorod surface. The surfactant bilayer makes nanorods positively charged and

stabilizes them in aqueous dispersions. For nanorods with AR = 4.4 at 20 nM concentration, the concentration of CTAB required to form a bilayer is estimated to be approximately 0.6 mM,[15] which is roughly in agreement with the experimental critical concentration. Au nanorods without the surfactant bilayer coating tend to aggregate in a disordered manner because of the large van der Waals attraction (Au–Au Hamaker constant $A \approx 1.95$ eV[42]). A minimum surfactant concentration is therefore required to maintain the balance between the entropic depletion potential and electrostatic repulsion potential for the formation of nanorod superstructures. Besides the surfactant concentration, the temperature at which the solvent evaporates is also important for the formation of ordered superstructures of Au nanorods. When the temperature is higher than approximately 60 °C, only disordered assemblies of Au nanorods form (Figure S5b in the Supporting Information), probably as solvent evaporation is too fast for Au nanorods to attain their equilibrium positions.

The droplet-evaporation technique has also been employed to produce ordered assemblies of Au nanostructures with other shapes, including polyhedra, nanocubes, and bipyramids. The resultant ordered assemblies are strongly shape-dependent, as revealed by SEM imaging (Figure 2) and their fast Fourier transforms (Figure S6 in the Supporting Information). Au polyhedra [diameter = (43 ± 1) nm, SPRW = 535 nm] assemble into a hexagonally packed superstructure. Au nanocubes [edge length = (50 ± 3) nm, SPRW = 545 nm] assemble into a tetragonally packed superstructure with nanocubes in different layers stacked on top of each other. Au bipyramids [middle diameter = (40 ± 4) nm, length = (185 ± 9) nm, AR = 4.6 ± 0.2, longitudinal SPRW = 1074 nm] have a pentagonal base in the middle and two sharp apexes at the ends.[40,41] When the CTBAB concentration is above roughly 5 mM, Au bipyramids assemble into either the nematic or 3D ordered superstructures (Figure S7 in the Supporting Information). When the CTBAB concentration is below this value, they mainly assemble into the nematic superstructure. The 3D ordered superstructure of Au bipyramids exhibit positional ordering along several different directions, as indicated by the fast Fourier transform. It can therefore be thought of as a 3D superlattice. The formation of a bipyramid superlattice, instead of the smectic-A superstructure formed by Au nanorods, can presumably be ascribed to the nonuniform diameter of bipyramids along their length axis. In addition, we believe that the role of CTBAB in the formation of bipyramid superstructures is similar to that of CTAB.

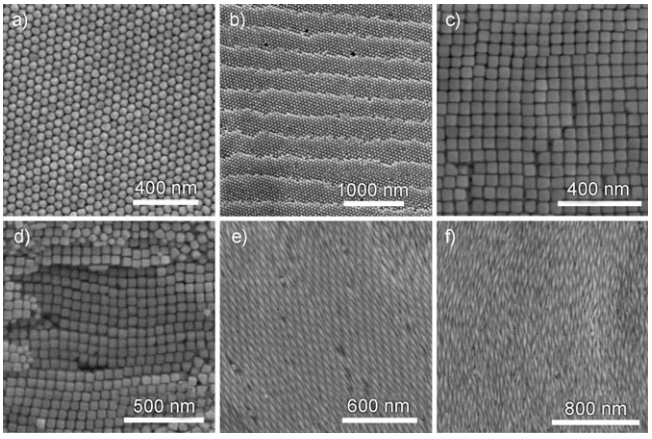

Figure 2. SEM images showing the ordered assemblies formed from differently shaped Au nanostructures: a) Hexagonally packed Au polyhedra; b) hexagonally packed Au polyhedra with approximately periodic monosteps; c) tetragonally packed Au nanocubes; d) steps showing that Au nanocubes in different layers are stacked on top of each other; e) 3D ordered superstructure formed from Au bipyramids when the cetyltrimethylammonium bromide (CTAB) concentration is approximately 10 mM; f) nematic superstructure formed from Au bipyramids when the CTBAB concentration is approximately 2 mM.

The phase behavior of mixtures of colloidal particles with different sizes and shapes has important implications for many industries, such as the production of paints and pigments. However, experimental studies of mixtures of anisotropic colloidal particles have remained relatively unexplored despite their wide range of applications.[43–45] We employed the droplet-evaporation technique to investigate the assemblies of the binary mixtures of Au nanostructures at a molar ratio of nearly 1:1. Two more Au nanorod samples were prepared by selective shortening,[35,37] wherein the nanorod diameter remained unchanged, whereas the nanorod length was selectively reduced. The two Au nanorod samples with AR = 4.4 and 3.8 were used as starting nanorods. The average diameter, length, AR, and longitudinal SPRW of one of the resultant nanorod samples were (16 ± 2) nm, (64 ± 5) nm, 4.0 ± 0.4, and 804 nm, and those of the other sample were (11 ± 1) nm, (29 ± 2) nm, 2.6 ± 0.3, and 664 nm, respectively. All of the six binary combinations of four different nanorod samples were investigated. The nature of the assembled superstructures was found to be solely determined by the relative diameters of the two nanorod samples. When two nanorod samples had different average diameters, they self-separated from each other, and each formed its own smectic superstructure (Figure 3 and Figure S8 in the Supporting Information, four cases). With two nanorod samples of equal average diameter, mixing occurred to form the nematic superstructure without self-separation (Figure S9 in the Supporting Information, two cases).

The droplet-evaporation technique has been further applied to the binary mixture of Au nanorods (AR = 4.4) and polyhedra. When the CTAB concentration in the dispersions of the binary mixture is adjusted between approximately 1 and 5 mM, an ordered superstructure of alternating Au nanorods and polyhedra is obtained (Figure 4). In this superstructure, Au polyhedra form a two-dimensional rectangular lattice within the same layer. Au polyhedra are nearly close-packed along one of the two perpendicular lattice directions. The distance between neighboring polyhedra along the other direction is enlarged by interposed Au nanorods. Moreover, the position occupied by each polyhedron in one layer corresponds to the center of the rectangular unit cell of the neighboring layer. This unusual alternating ordered superstructure forms only under appropriate CTAB concentrations. Au nanorods and polyhedra self-separate when the CTAB concentration is higher than approximately 5 mM, and they form disordered mixtures

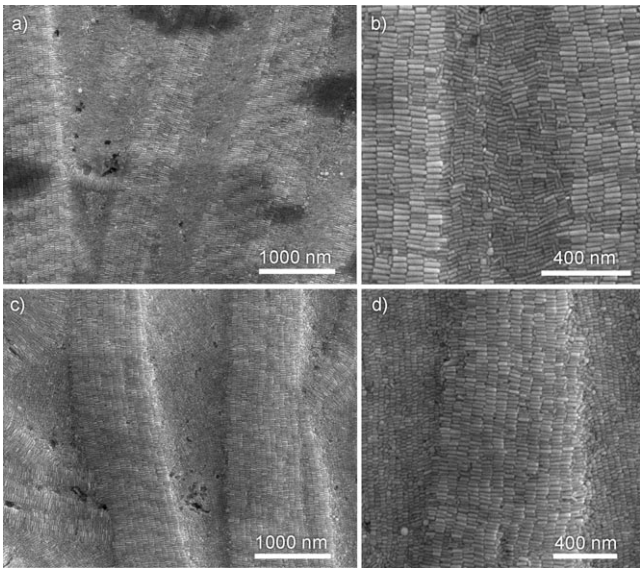

Figure 3. SEM images showing the self-separation and superstructure formation of binary mixtures of differently sized Au nanorods. a, b) Mixture of Au nanorods with ARs of 4.4 and 3.8. c, d) Mixture of Au nanorods with ARs of 4.0 and 2.6. Each nanorod sample forms the smectic superstructure.

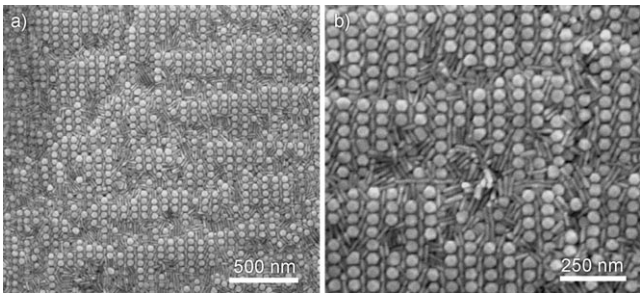

Figure 4. a) SEM image of the ordered superstructure formed from the binary mixture of Au nanorods (AR = 4.4) and polyhedra; b) the same binary superstructure at higher magnification.

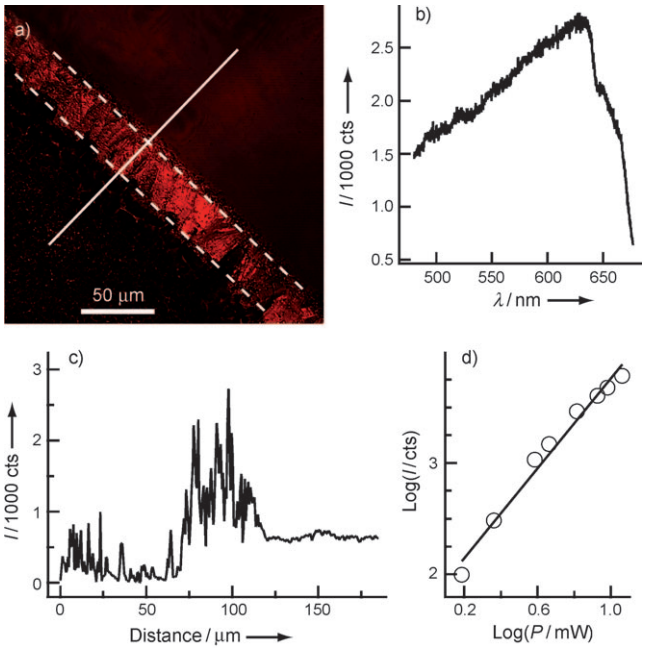

Figure 5. Enhanced two-photon-excited luminescence from ordered Au nanorod (AR = 4.4) superstructures: a) Confocal two-photon-excited luminescence image. The ring annulus is indicated by the parallel dashed lines; b) two-photon-excited luminescence spectrum taken from ordered Au nanorod assemblies; c) representative trace of the two-photon-excited luminescence intensity versus distance taken along the solid line shown in (a). The smooth plateau on the right side is the two-photon-excited luminescence signal from the silicon substrate; d) dependence of the luminescence intensity on the excitation power. The slope determined from linear fitting is (2.0 ± 0.1), indicating two-photon-excited luminescence.

when the CTAB concentration is lower than about 1 mM (Figure S10 in the Supporting Information).

Gold nanorods have been demonstrated to exhibit interesting two-photon-excited photoluminescence properties[46,47] and used as bright contrast agents for two-photon-excited luminescence imaging of mouse ear blood vessels[48] and cancer cells in 3D tissue phantoms down to 75 μm deep.[49] We have measured the two-photon-excited luminescence from the ordered superstructures of Au nanorods using confocal laser scanning microscopy (Figure 5). Two-photon-excited luminescence is confirmed by the quadratic dependence of the luminescence intensity on the excitation power (Figure 5c). Luminescence images (Figure 5a) and intensity profiles (Figure 5d) show that the two-photon-excited luminescence of ordered Au nanorod superstructures in the ring annulus is approximately six times stronger than that of disordered nanorod assemblies inside the ring. In comparison, the luminescence intensity of disordered nanorod assemblies produced by evaporation at higher temperatures in the ring annulus is nearly equal to that of nanorod assemblies inside the ring (Figure S11 in the Supporting Information). In addition, for the nanorods of AR = 4.4, the surface number density of exposed nanorods in the ring annulus for ordered assemblies [(670 ± 10) μm^{-2}] is only slightly larger than that for disordered assemblies [(550 ± 30) μm^{-2}]. These results suggest that the enhanced luminescence intensity from ordered nanorod superstructures is not due to the larger amount of nanorods in the ring annulus. We believe that the enhanced luminescence results from plasmon coupling among well-ordered Au nanorods. Larger luminescence enhancements can be expected if the excitation wavelength matches with the coupled plasmon-resonance wavelength of ordered nanorod superstructures.

In summary, we have demonstrated the formation of large-area, 3D ordered assemblies of Au nanostructures of different sizes and shapes, including nanorods, polyhedra, nanocubes, and bipyramids, by droplet evaporation. The optimal particle concentration, surfactant concentration, and evaporation temperature ranges for the formation of ordered superstructures were 10–30 nM, 1–10 mM, and room temperature to approximately 60 °C, respectively. The nature of the resultant assemblies was strongly dependent on the shape of Au nanostructures for single-component systems. Nanorods, polyhedra, nanocubes, and bipyramids formed nematic/smectic, hexagonally packed, tetragonally packed, and nematic/3D ordered superstructures, respectively. Binary mixtures of Au

nanorods of different sizes either assembled into nematic superstructures or self-separated, with each nanorod sample forming its own smectic superstructure. The assembly of binary nanorod mixtures was dependent on the relative diameters of two nanorod samples for the nanorods used in our experiments. Moreover, binary mixtures of Au nanorods and polyhedra assembled into an alternating ordered superstructure. The two-photon-excited luminescence of ordered nanorod assemblies was enhanced compared to that for disordered nanorod assemblies. We believe that the droplet-evaporation technique can be extended to other anisotropic nanostructured materials for the fabrication of large-scale ordered superstructures with interesting physical properties.

Experimental Section

Gold nanostructures of different shapes and sizes were prepared using a seeded growth method with ammonium surfactants as stabilizing agents. Specifically, Au nanorods with ARs of 4.4 and 3.8 were prepared according to the procedures reported previously.[35,36] Anisotropic oxidation of these two nanorod samples afforded Au nanorods with ARs of 4.0 and 2.6, respectively.[35,37] Au nanocubes and polyhedra were synthesized according to the method developed by Sau and Murphy.[38,39] Au bipyramids with an AR of 4.6 were made according to our reported method.[41] More details are provided in the Supporting Information.

As-prepared Au nanostructures were processed by centrifugation (10000 rpm, 9800 g, 10 min) and re-dispersion into water to maintain a stabilizing surfactant concentration of 0.1–10 mM and a particle concentration of 10–30 nM. For the preparation of Au nanostructure assemblies, a drop (5–10 μL) of the processed dispersion of Au nanostructures was placed onto a clean silicon substrate. The sessile droplet was kept still at room temperature under approximately 60% humidity over about 8 h for evaporation of water. After evaporation, a ring, made up of Au nanostructure assemblies, was observed on the substrate. For the preparation of assemblies out of binary mixtures of Au nanostructures, equal volumes of dispersions in water of two types of Au nanostructure, at similar particle concentrations, were mixed together. One drop (5–10 μL) of the mixture was cast onto a silicon substrate for evaporation.

SEM imaging was performed on a FEI Quanta 400 FEG microscope. Transmission electron microscopy imaging was carried out on a FEI CM120 microscope to measure the size distributions of Au nanostructures. Extinction spectra were recorded using a Hitachi U-3501 UV/Vis/NIR spectrophotometer to determine SPRW values. The thicknesses of Au nanostructure assemblies were measured using an Alpha-Step 500 surface profiler. Two-photon-excited luminescence measurements were performed on an Olympus FV300-IX71 confocal laser scanning microscope integrated with an Acton SpectroPro 2150i monochromator and a Princeton Instruments liquid nitrogen-cooled Spec-10:100B charge-coupled device. The excitation light from a Coherent Mira 900B mode-locked Ti-sapphire laser system (pulse duration = 100 fs, repetition rate = 76 MHz, wavelength = 800 nm) was focused by a water-immersion objective (60×, numerical aperture = 1.2) to a spot of approximately 1 μm in diameter. The laser power on the sample during scanning was 11.5 mW. A band-pass filter (585–640 nm) was employed for imaging, and a short-pass filter (cut-on wavelength = 750 nm) was used for spectral measurements.

Received: July 25, 2008
Published online: November 10, 2008

Keywords: gold · luminescence · nanostructures · self-assembly · surfactants

[1] F. M. van der Kooij, K. Kassapidou, H. N. W. Lekkerkerker, *Nature* **2000**, *406*, 868–871.
[2] A. E. Saunders, A. Ghezelbash, D.-M. Smilgies, M. B. Sigman, Jr., B. A. Korgel, *Nano Lett.* **2006**, *6*, 2959–2963.
[3] F. Livolant, A. M. Levelut, J. Doucet, J. P. Benoit, *Nature* **1989**, *339*, 724–726.
[4] Z. Dogic, S. Fraden, *Phys. Rev. Lett.* **1997**, *78*, 2417–2420.
[5] M. Li, H. Schnablegger, S. Mann, *Nature* **1999**, *402*, 393–395.
[6] H. Maeda, Y. Maeda, *Phys. Rev. Lett.* **2003**, *90*, 018303.
[7] S. Meuer, P. Oberle, P. Theato, W. Tremel, R. Zentel, *Adv. Mater.* **2007**, *19*, 2073–2078.
[8] A. Dessombz, D. Chiche, P. Davidson, P. Panine, C. Chanéac, J.-P. Jolivet, *J. Am. Chem. Soc.* **2007**, *129*, 5904–5909.
[9] L.-S. Li, J. Walda, L. Manna, A. P. Alivisatos, *Nano Lett.* **2002**, *2*, 557–560.
[10] L.-S. Li, A. P. Alivisatos, *Adv. Mater.* **2003**, *15*, 408–411.
[11] D. V. Talapin, E. V. Shevchenko, C. B. Murray, A. Kornowski, S. Förster, H. Weller, *J. Am. Chem. Soc.* **2004**, *126*, 12984–12988.
[12] A. Ghezelbash, B. Koo, B. A. Korgel, *Nano Lett.* **2006**, *6*, 1832–1836.
[13] L. Onsager, *Ann. N. Y. Acad. Sci.* **1949**, *51*, 627–659.
[14] B. Nikoobakht, Z. L. Wang, M. A. El-Sayed, *J. Phys. Chem. B* **2000**, *104*, 8635–8640.
[15] N. R. Jana, L. A. Gearheart, S. O. Obare, C. J. Johnson, K. J. Edler, S. Mann, C. J. Murphy, *J. Mater. Chem.* **2002**, *12*, 2909–2912.
[16] N. R. Jana, *Angew. Chem.* **2004**, *116*, 1562–1566; *Angew. Chem. Int. Ed.* **2004**, *43*, 1536–1540.
[17] T. K. Sau, C. J. Murphy, *Langmuir* **2005**, *21*, 2923–2929.
[18] Z.-C. Xu, C.-M. Shen, C.-W. Xiao, T.-Z. Yang, S.-T. Chen, H.-L. Li, H.-J. Gao, *Chem. Phys. Lett.* **2006**, *432*, 222–225.
[19] R. D. Deegan, O. Bakajin, T. F. Dupont, G. Huber, S. R. Nagel, T. A. Witten, *Nature* **1997**, *389*, 827–829.
[20] R. D. Deegan, *Phys. Rev. E* **2000**, *61*, 475–485.
[21] H. Hu, R. G. Larson, *Langmuir* **2005**, *21*, 3963–3971.
[22] S. Maheshwari, L. Zhang, Y. X. Zhu, H.-C. Chang, *Phys. Rev. Lett.* **2008**, *100*, 044503.
[23] I. I. Smalyukh, O. V. Zribi, J. C. Butler, O. D. Lavrentovich, G. C. L. Wong, *Phys. Rev. Lett.* **2006**, *96*, 177801.
[24] R. van Hameren, et al., *Science* **2006**, *314*, 1433–1436.
[25] Z. Q. Lin, S. Granick, *J. Am. Chem. Soc.* **2005**, *127*, 2816–2817.
[26] J. Xu, J. F. Xia, S. W. Hong, Z. Q. Lin, F. Qiu, Y. L. Yang, *Phys. Rev. Lett.* **2006**, *96*, 066104.
[27] D. J. Harris, H. Hu, J. C. Conrad, J. A. Lewis, *Phys. Rev. Lett.* **2007**, *98*, 148301.
[28] S. Narayanan, J. Wang, X.-M. Lin, *Phys. Rev. Lett.* **2004**, *93*, 135503.
[29] J. X. Huang, F. Kim, A. R. Tao, S. Connor, P. D. Yang, *Nat. Mater.* **2005**, *4*, 896–900.
[30] T. P. Bigioni, X.-M. Lin, T. T. Nguyen, E. I. Corwin, T. A. Witten, H. M. Jaeger, *Nat. Mater.* **2006**, *5*, 265–270.
[31] N. Lu, et al., *Nano Lett.* **2004**, *4*, 885–888.
[32] J. Xu, J. F. Xia, Z. Q. Lin, *Angew. Chem.* **2007**, *119*, 1892–1895; *Angew. Chem. Int. Ed.* **2007**, *46*, 1860–1863.
[33] C. Querner, M. D. Fischbein, P. A. Heiney, M. Drndić, *Adv. Mater.* **2008**, *20*, 2308–2314.
[34] Q. W. Li, Y. T. Zhu, I. A. Kinloch, A. H. Windle, *J. Phys. Chem. B* **2006**, *110*, 13926–13930.
[35] W. H. Ni, X. S. Kou, Z. Yang, J. F. Wang, *ACS Nano* **2008**, *2*, 677–686.
[36] X. S. Kou, S. Z. Zhang, Z. Yang, C.-K. Tsung, G. D. Stucky, L. D. Sun, J. F. Wang, C. H. Yan, *J. Am. Chem. Soc.* **2007**, *129*, 6402–6404.

[37] C.-K. Tsung, X. S. Kou, Q. H. Shi, J. P. Zhang, M. H. Yeung, J. F. Wang, G. D. Stucky, *J. Am. Chem. Soc.* **2006**, *128*, 5352 – 5353.
[38] T. K. Sau, C. J. Murphy, *J. Am. Chem. Soc.* **2004**, *126*, 8648 – 8649.
[39] H. J. Chen, X. S. Kou, Z. Yang, W. H. Ni, J. F. Wang, *Langmuir* **2008**, *24*, 5233 – 5237.
[40] X. S. Kou, S. Z. Zhang, C.-K. Tsung, M. H. Yeung, Q. H. Shi, G. D. Stucky, L. D. Sun, J. F. Wang, C. H. Yan, *J. Phys. Chem. B* **2006**, *110*, 16377 – 16383.
[41] X. S. Kou, W. H. Ni, C.-K. Tsung, K. Chan, H.-Q. Lin, G. D. Stucky, J. F. Wang, *Small* **2007**, *3*, 2103 – 2113.
[42] D. Bargeman, F. van Voorst Vader, *J. Electroanal. Chem.* **1972**, *37*, 45 – 52.
[43] S. M. Oversteegen, J. G. E. J. Wijnhoven, C. Vonk, H. N. W. Lekkerkerker, *J. Phys. Chem. B* **2004**, *108*, 18158 – 18163.
[44] S. M. Oversteegen, C. Vonk, J. E. G. J. Wijnhoven, H. N. W. Lekkerkerker, *Phys. Rev. E* **2005**, *71*, 041406.
[45] N. Miyamoto, Y. Yamada, S. Koizumi, T. Nakato, *Angew. Chem.* **2007**, *119*, 4201 – 4205; *Angew. Chem. Int. Ed.* **2007**, *46*, 4123 – 4127.
[46] K. Imura, T. Nagahara, H. Okamoto, *J. Am. Chem. Soc.* **2004**, *126*, 12730 – 12731.
[47] A. Bouhelier, R. Bachelot, G. Lerondel, S. Kostcheev, P. Royer, G. P. Wiederrecht, *Phys. Rev. Lett.* **2005**, *95*, 267405.
[48] H. F. Wang, T. B. Huff, D. A. Zweifel, W. He, P. S. Low, A. Wei, J.-X. Cheng, *Proc. Natl. Acad. Sci. USA* **2005**, *102*, 15752 – 15756.
[49] N. J. Durr, T. Larson, D. K. Smith, B. A. Korgel, K. Sokolov, A. Ben-Yakar, *Nano Lett.* **2007**, *7*, 941 – 945.

